Grenze International Journal of Engineering and Technology, June Issue

Development of Automatic Segmentation Techniques using Convolutional Neural Networks to Differentiate Brain Tumors

Dr. Prathibha G[1] and Ms. Sindhu Jain A M[2]
[1-2]Rajeev Institute of Technology/ Department of ISE, Hassan, India
Email: prathibhaghebbar@rithassan.ac.in, sindhujainam96@gmail.com

Abstract*—Image feature extraction strategies are utilized in computer vision to extricate features that are then learned for classification errands. The determination of a particular component extractor from among the many element extractors accessible in biomedical pictures is not just erratic, yet it likewise requires time to decide the best boundaries for a specific element extraction strategy. The Grey-level co-occurrence matrix (GLCM) feature extractor for using a random forest classifier to classify MRI images of brain cancer is the primary focus of this work. The accuracy, true positive rate, true negative rate, false positive rate, and false negative rate derived from the confusion matrix were used to assess the viability of GLCM features on random forest classification using a dataset of 245 brain MRI images divided into two classes: images with tumor (154 images) and images without tumor (91 images). The findings demonstrate that a significant texture component in brain MRI images is effectively removed by the GLCM feature while exhibiting promising accuracy and other execution measures. By including the neighbourhood free into the outdated classification model, a new classification system is implied. When calculating neighbourhood autonomous projections for LIPC, region is important. In determining whether neighbourhood anchor implanting is more effective at settling linear projection loads than other coding techniques, region is also taken into consideration. Additionally, LIPC takes information dispersion across different classes into account by training a softmax regression model, which can improve classification execution. In this study, 40 brain tumour MRI images without ground truth information were ulitilzed as testing data, and 80 brain tumour MRI images with ground truth data were used as training information. An online assessment tool evaluates the segmentation results of testing information. On genuine patient information, the proposed system method's typical dice similarities for segmenting whole tumor, tumour core, and contrast-enhancing tumour are 0.84, 0.685, and 0.585, respectively. These outcomes are similar to those of other cutting-edge methods.

***Index Terms*— MRI, Brain tumor, GLCM.**

I. INTRODUCTION

Cells that develop in an ill-advised way cause brain tumours [1]. The brain tumours may be benign or malignant, similar as different tumours. Regularly, a malignant tumour spreads quicker than a benign tumour [2]. Essential brain tumours are those that begin in the brain, while optional brain tumours are those that spread to the brain

Grenze ID: 01.GIJET.9.2.422

from different regions of the body. Brain tumour side effects could fluctuate from one individual to another; however, a portion of the incessant ones incorporate queasiness, regurgitating, migraines, seizures, and loss of equilibrium, among others. Despite the fact that there are various types of brain tumours, gliomas, meningiomas, and medulloblastomas are the most pervasive ones [3].

Brain tumours occur as a result of abnormal cell growth [1]. The brain tumours might be benign or malignant, just as other tumours. Typically, a malignant tumour spreads faster than a benign tumour [2]. The term "essential brain tumour" refers to a tumour that starts in the brain stem; the term "optional brain tumour" refers to a tumour that spreads to the brain stem from other sections of the body. The unfriendly impacts of a brain tumour fluctuate from one individual to another, but a few normal side symptoms include nausea, regurgitation, migraines, seizures, loss of equilibrium, and so on. Although there are many other types of brain tumors, gliomas, meningiomas, and medulloblastomas are the most well-known types [3]. The gliomas brain tumour may be a lowgrade astrocytoma, a slow-growing growth that is frequently benign, or a glioblastoma multiforme, a fast-growing growth that is usually malignant [4]. The meningioma often starts in the brain and is benign. The prevalence of medulloblastoma is higher in children than in adults [5]. The radiologists and oncologists are assisted by brain tumour imaging modalities prior to treatment (to assess the lesion degree, review), during treatment (to depict), and following treatment (to assess the response to therapy, check) [6]. Mass spectroscopy, brain perfusion (CT and MRI), dispersion tensor imaging (DTI), practical magnetic resonance imaging (fMRI), and other techniques are used to image brain tumours [7]. A very powerful magnet and radio waves are used in magnetic resonance imaging (MRI) to create images of the brain [8]. Before getting an MRI, all metal objects should be put away because they slow down the magnetic field and produce false signals. The radiologist occasionally uses elective imaging techniques on patients who have metallic implants like pacemakers. The MRI imagers are closed-type open-type. The image quality obtained with open-type MRI scanners is not as good as that obtained with closed-type MRI scanners [9]. A powerful magnetic field is produced by the magnet, and radio waves are sent into the brain using rf coils. The MRI imager uses the body's energy signals after the radio waves have stopped to capture a picture of the brain [10]. In order to improve the image's distinction, the MRI scans are occasionally taken using a dye. The organisation is as follows, about the relevant work in Section II. The dataset and method are presented in Section III. The results and comments are presented in Section IV. The task is concluded in Section V.

II. Related Work

The testing task is the automated detection of tumours in clinical photographs. For the recognition results to be extremely precise, the feature segment and classifier choice are crucial. A two-layered artificial neural network has been used to classify brain tumours using the highlights obtained from the grey-level co-occurrence matrix [11]. The approach yielded an accuracy of 97.5%. Four categories—astrocytoma, meningioma, metastatic bronchogenic cancer, and sarcoma—are used to categorise the images of the brain. In consideration of correlation, contrast, divergence, energy, homogeneity, variance, and entropy, a total of 16 elements are separated. The evolutionary algorithm is used to use the contingent entropy [12].

Using texture highlights obtained from GLCM and wavelets, the segmentation and classification of brain tumours have been completed. The Otsu thresholding approach is used to segment the brain MRI images, and k-means clustering is then carried out. The texture components are obtained via GLCM, and wavelets are used to eliminate highlights. Prior to using support vector machines to classify the images, the consolidated elements are passed to PCA. For the classification of brain MRI images, it has been demonstrated that linear kernels perform better than polynomial kernels [13]. Utilizing highlights for texture and contour, image recovery is done [14]. Using various components obtained from GLCM and kernel support vector machines as a classifier, brain MRI images are sorted. After extracting the highlights, the element reduction module is used before submitting the elements to the kernel support vector machines for classification [16]. Using schematic segmentation and support vector machine-based classification of highlights extracted from grey-level co-occurrence matrix, the clustering of brain tumour MRI images is completed [17]. The preprocessing of the photos makes use of median filtering. The method is shown to have a classification accuracy of 93.05%.

III. Methodology

For image classification, the highlights are Scale Invariant Feature Transform (SIFT), Speeded-Up Robust Features (SURF), and Oriented FAST and Rotated BRIEF (ORB) [18]. To create an element vector that addresses the restricted area surrounding the component point, these component extractors separate geometric,

color, textural, and shape data. SIFT is a 128-dimensional feature vector that can withstand loud sensor cacophony, many relative shifts, and brightness changes [19]. Fig. 1 shows the SIFT features that were derived from the MRI scans of the cerebrum tumour. SIFT has not been used in this work because computing SIFT highlights for brain tumour MRI image classification is computationally expensive due to the 128 components of SIFT and the large number of such elements in a single image.

The venture proposes a segmenting and detecting tumor by involving spatial fuzzy clustering algorithm for Magnetic Resonance (MRI) images to identify the Brain Tumor. By including the neighbouring free projection into the established classification model, a new classification system is established. The assessment of neighbouring free projections for LIPC considers area. The phases of a brain tumour are classified using an artificial neural network, which is subsequently trained. Morphologic items of MRI now and again require segmentation of the image volume into tissue types.

Additionally, manual segmentation reveals significant inter- and intra-observer variation. For instance, the examination of numerous brain issues is interested in the precise segmentation of MR images of the brain. Preprocessing, feature extraction, tumour segmentation using the LIPC approach, and postprocessing make up the four key stages of the suggested procedure. We implemented the suggested technique in a multiresolution system to reduce computing costs. the arbitrary results of combining the suggested method with the mastered softmax regression model on different information collections. For each class at each level, parameters k, N, and w were set to 10, 40 000, and 5, respectively. Compared to the manufactured information, the tumour boundaries of the actual patient data were more hazy. In this approach, the manufactured information was chosen above the actual patient information for the tumour categorization execution. There were more incorrectly identified voxels in the edoema localities than there were in the tumour regions due to the extremely hazy edoema limits of both real patient information and made-up information. Two further regular segmentation outcomes using the suggested method. that low-grade genuine patient information's tumour boundary was hazier than that of high-grade genuine patient information.

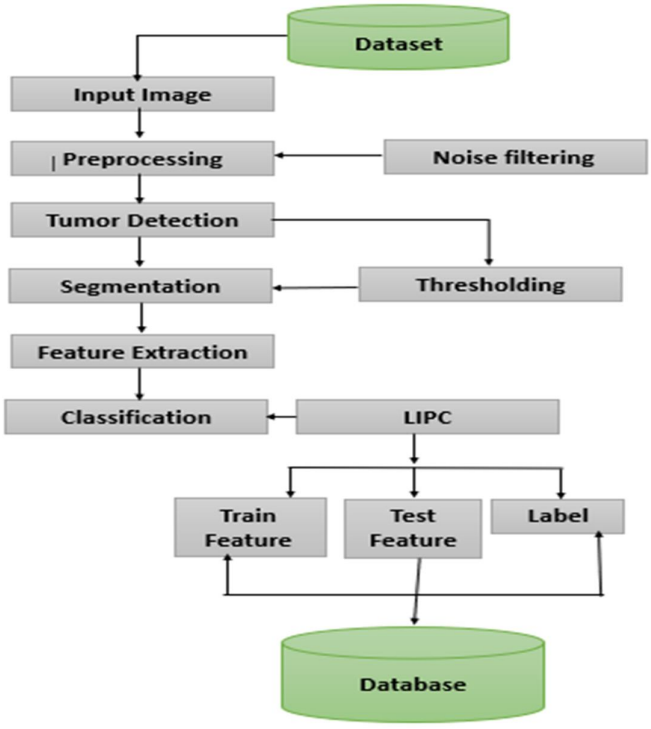

Figure 1. Proposed Methodology

Second-rate real patient data in the edoema area was also hazy. As a result, the tumour and edoema classification accuracy in the low-grade patient information was lower than that in the high-grade patient information. LAE was used as the coding approach in both SRC and LIPC to evaluate the suitability of LIPC. The classification scores were also recorded. For LIPC, the variables k, N, and w were set to 10, 40 000, and 5 for each class at

each level, respectively. A word reference for SRC was created for each level and contains tests from three different classes. This word reference included three subdictionaries, each of which connected to a particular class. The size of each subword referrence was set to 40 000 to ensure a fair test. Subsequently,The word reference size for SRC was 120 000 words at each level as a result.The number of nonzero values for SRC in LAE was decided upon as follows. We randomly selected 10,000 examples from the preparation data for each class at each level before using the word reference to compute the recreation mistake standards for all the selected tests. In LAE, there were between 5 and 1,200 nonzero values. The base remaking error was finally discovered when the number of nonzero numbers was increased to 1000. The mean DS of LIPC was 5.3% higher than that of SRC after we looked at the effects of various information gatherings. The classification outcomes using LIPC and SRC on different information bundles are displayed, demonstrating the potential usefulness of the proposed LIPC for tumour segmentation.

A. Advantage

1. The principal benefit of this process is the identifying the tumor region, thus it is more useful for the simple conclusion.
2. The exactness of the segmentation is worked on because of the thresholding.
3. This strategy is prevalent when contrasted with SVM classifier.

B. Dataset Used

MRI pictures of a brain tumour make up the dataset. There are 245 photos in all. There are 154 photos with tumors, while there are only 91 images without tumours. The dataset is 7.22 MB in size. The collection contains a variety of image sizes; for example, some photos have a spatial resolution of 300x168 while others have a resolution of 200x200. The information size is also not uniform, with some of the photos being 4.46 KB and others being 5.76 KB. The photos in the dataset are organised in jpg format. For the MRI images of the brain tumor, the quantifiable texture features were obtained via GLCM.

1)Energy feature: The square root of the angular second moment feature is the energy feature. This element deals with the texture of the image's consistency. (1) provides the energy feature obtained from the GLCM. Since GLCM is a standardised matrix, solidarity is the thing that the energy is worth most.

$$E = \sqrt{\sum \sum \{(i, j)\}}\ N{-}1\ 2\ j{=}0\ N{-}1\ i{=}0\ \ldots\ldots\ldots\ldots(1)$$

2) Dissimilarity Feature: The disparity takes into account the texture of the image's heterogeneity. By replicating the GLCM cell values with straight loads in accordance with (2), the dissimilarity characteristic may be obtained.

$$D = \sum \sum |i - j\ N{-}1\ j{=}0\ N{-}1\ i{=}0\ |(i, j)\ \ldots\ldots\ldots(2)$$

3) Homogeneity Feature: Huge upsides values of the diagonal components of the GLCM are used to address the large uniformity in the image texture. The homogeneity is highest when the image pixel values are constant. Significant difference reduces the image's uniformity. (3) provides the homogeneity characteristic.

$$\mathrm{H} = \sum \sum P(i,j)\ 1{+}(i{-}j)\ 2\ N{-}1\ j{=}0\ N{-}1\ i{=}0\ \ldots\ldots\ldots(3)$$

4) Contrast Feature: A measure of distinction between the lowest and largest pixel values in a group of pixels is the contrast feature. The feature of contrast is provided by (4).

$$H = \sum \sum (i, j)(i - j)\ 2\ N{-}1\ j{=}0\ N{-}1\ i{=}0\ \ldots\ldots\ldots(4)$$

By separating these four highlights for various upsides of offset and angles, an element vector is obtained. The image is taken with a stage size of 1 and 3 pixels at an angle of 0, 45, and 900 degrees. To categorise the MRI pictures of brain tumors, a classifier is given the learned highlights. Some common classifiers used for image classification tasks include decision trees, support vector machines, k-nearest neighbor, and random forests. In this study, we used a random forest classifier to categorise MRI scans of brain tumours. The purpose of the other quantifiable tests, such as the Chi-square test and t-tests, is to determine whether the strategy is adequate.

IV. Results Obtained

The accompanying figures 2, 3, 4 and 5 shows the different methods involved during the time spent in determination of brain tumor.

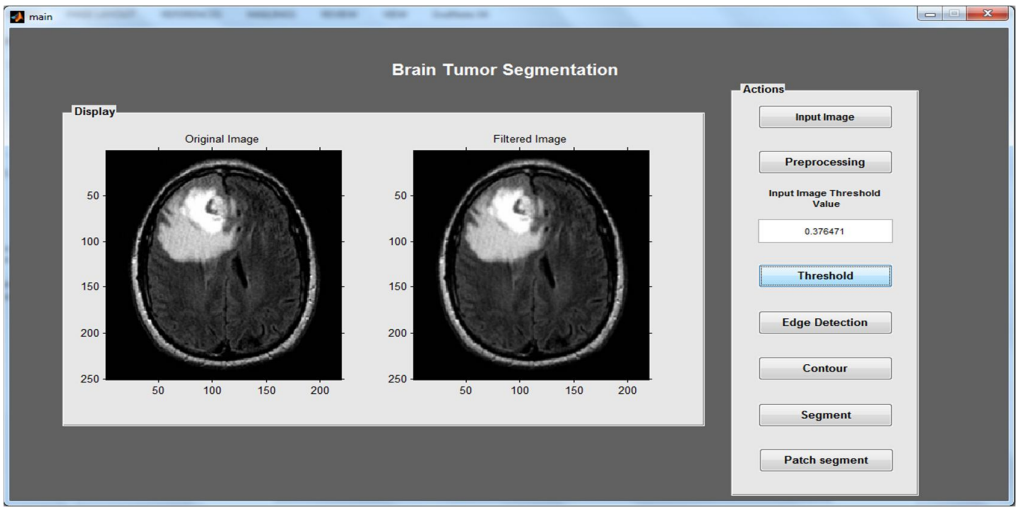

Figure 2. Brain tumour segmentation showing filtered image, Preporocessing, and Thresholdong

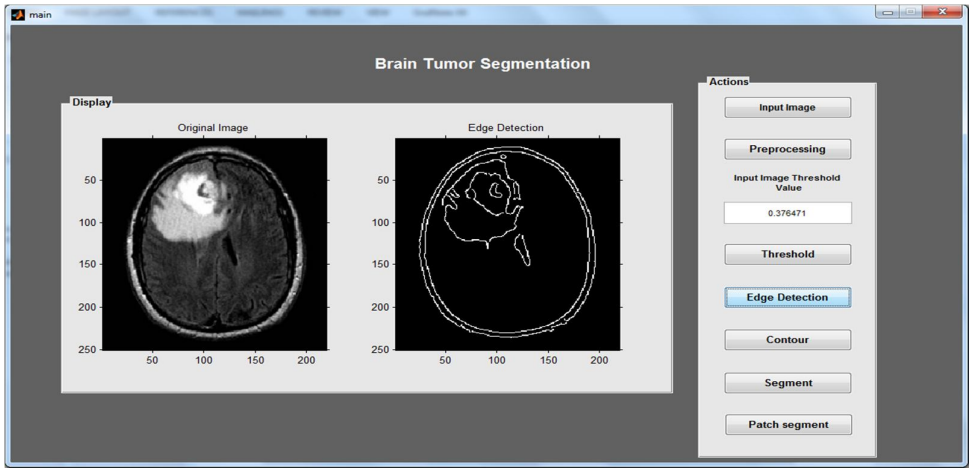

Figure 3. Brain tumour segmentation showing edge detection using canny edge detector

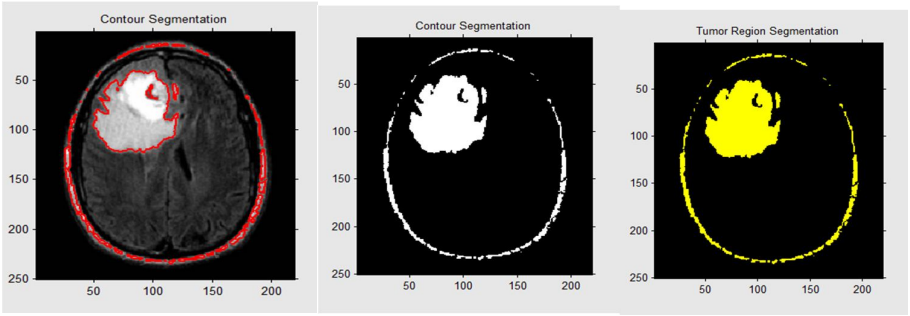

Figure 4. Illustration of different contour segmentations and Tumor region segmentation

Confusion Matrix:

A confusion matrix is available to evaluate the effectiveness of the method. In Fig. 6, the confusion matrix is displayed. The confusion matrix demonstrates that there is no anticipated class "no" that is actually "yes." There were 18 photos tested in all. Nine of the 18 photos fall under the 'yes' category, while nine fall under the 'no' category.

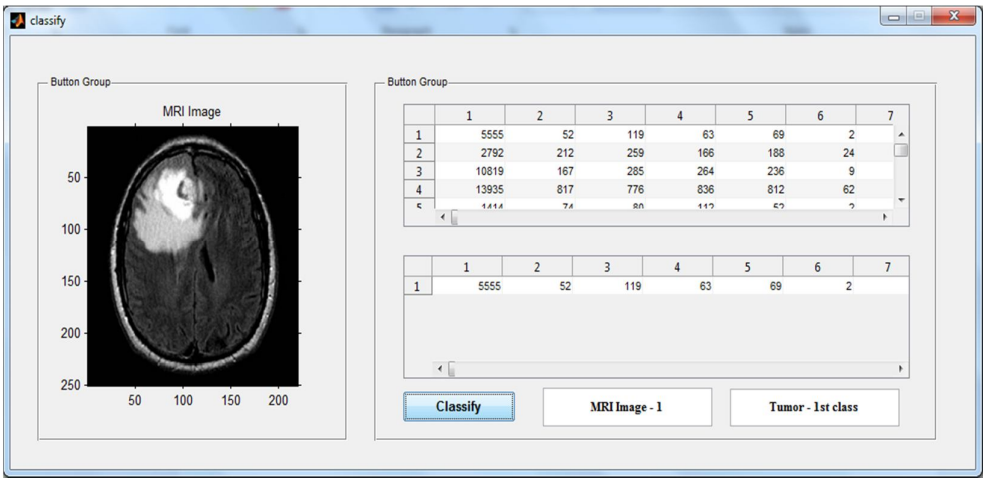

Figure 5. Results shows the MRI image as Tumour 1st Class

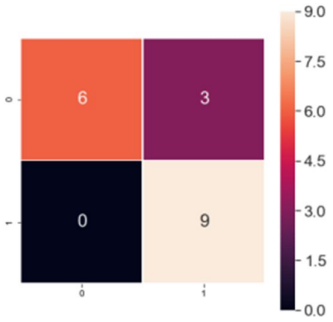

Fig. 6. Confusion matrix

V. Conclusion

As a result, we introduce a unique technique to segment MRI brain tumours and categorise whether an image is common or unusual. According on simulation findings, our Classifier and segmentation outperform alternative methods. For the purpose of segmenting brain tumours in MRI images, a programmed strategy is suggested. To address the tumour segmentation problem, a LIPC-based approach was learned. The traditional classification model was integrated with the proposed LIPC's adjacent free projection, and a new classification framework was established. The LAE technique was superior to other coding methods for settling the linear reconstruction weights under the area restriction. We utilized a softmax model to understand the relationship between the information dissemination and recreation blunder standard since the information dispersion in each sub complex was crucial for classification. We assessed the recommended strategy utilizing both fabricated data and freely available imaging data of brain tumours. Our method outperformed rival tactics in the two cases.

Brain tumour MRI scans are divided into two classes: those with and those without tumours. When compared to SIFT features, the grey-level co-occurrence matrix obtained from the brain tumour MRI images provides quantifiable texture highlights that are computationally quick. On a small dataset, the random forest classifier successfully categorises the photos with an accuracy of 83.3%. Applying certain pre-handling techniques to the photographs could enhance the technique's demonstration. To increase the precision, GLCM features could be used with another component extraction technique. The method can be implemented by adding additional model layers.

References

[1] Surawicz, Tanya S., et al. "Brain tumor survival: results from the National Cancer Data Base." Journal of neuro-oncology 40.2 (1998): 151-160.

[2] Albini, A., et al. "A rapid in vitro assay for quantitating the invasive potential of tumor cells." Cancer research 47.12

(1987): 3239-3245.
[3] Waage, Ingunn Syversen, Ingeborg Vreim, and Sverre Helge Torp. "Cerb B2/HER2 in Human Gliomas, Medulloblastomas, and Meningiomas: a Minireview." International journal of surgical pathology 21.6 (2013): 573-582.
[4] A. K. Aggarwal, "GPS-Based Localization of Autonomous Vehicles," Autonomous Driving and Advanced Driver-Assistance Systems (ADAS): Applications, Development, Legal Issues, and Testing, p. 437, 2021.
[5] Mathew, A. Reema, P. Babu Anto, and N. K. Thara. "Brain tumor segmentation and classification using DWT, Gabour wavelet and GLCM." 2017 International Conference on Intelligent Computing, Instrumentation and Control Technologies (ICICICT). IEEE, 2017.
[6] A. Kaur, A. P. S. Chauhan, and A. K. Aggarwal, "An automated slice sorting technique for multi-slice computed tomography liver cancer images using convolutional network," Expert Systems with Applications, vol. 186, p. 115686, 2021.
[7] Jellinger, K. "Glioblastoma multiforme: morphology and biology." Acta neurochirurgica 42.1 (1978): 5-32.
[8] Rochkind, Semion, et al. "Extracranial metastases of medulloblastoma in adults: literature review." Journal of Neurology, Neurosurgery & Psychiatry 54.1 (1991): 80-86.
[9] A. K. Aggarwal, "Biological Tomato Leaf Disease Classification using Deep Learning Framework," International Journal of Biology and Biomedical Engineering, vol. 16, no. DOI: 10.46300/91011.2022.16.30, pp. 241–244, 2022.
[10] Huang, Raymond Y., et al. "Pitfalls in the neuroimaging of glioblastoma in the era of antiangiogenic and immuno/targeted therapy–detecting illusive disease, defining response." Frontiers in neurology 6 (2015): 33.
[11] Dimou, S., et al. "A systematic review of functional magnetic resonance imaging and diffusion tensor imaging modalities used in presurgical planning of brain tumour resection." Neurosurgical review 36.2 (2013): 205-214.
[12] Katti, Girish, Syeda Arshiya Ara, and Ayesha Shireen. "Magnetic resonance imaging (MRI)–A review." International journal of dental clinics 3.1 (2011): 65-70.
[13] M. Garg, J. S. Ubhi, and A. K. Aggarwal, "Neural Style Transfer for Image within Images and Conditional GANs for Destylization," Journal of Visual Communication and Image Representation, 2022.
[14] Foster- Gareau, Paula, et al. "Imaging single mammalian cells with a 1.5 T clinical MRI scanner." Magnetic Resonance in Medicine: An Official Journal of the International Society for Magnetic Resonance in Medicine 49.5 (2003): 968-971.
[15] Armstrong, Peter, and Stephen F. Keevil. "Magnetic resonance imaging--1: Basic principles of image production." BMJ: British Medical Journal 303.6793 (1991): 35.
[16] Zulpe, Nitish, and Vrushsen Pawar. "GLCM textural features for brain tumor classification." International Journal of Computer Science Issues (IJCSI) 9.3 (2012): 354.
[17] Chauhan, Sumika, Manmohan Singh, and Ashwani Kumar Aggarwal. "An effective health indicator for bearing using corrected conditional entropy through diversity-driven multi-parent evolutionary algorithm." Structural Health Monitoring (2020): 1475921720962419.
[18] Arora, Kratika and Ashwani Kumar Aggarwal. "Approaches for Image Database Retrieval Based on Color, Texture, and Shape Features." Handbook of Research on Advanced Concepts in Real-Time Image and Video Processing, edited by Md. Imtiyaz Anwar, et al., IGI Global, 2018, pp. 28-50. http://doi:10.4018/978-1-5225-2848-7.ch002
[19] Jain, Shweta. "Brain cancer classification using GLCM based feature extraction in artificial neural network." International Journal of Computer Science & Engineering Technology 4.7 (2013): 966-970.
[20] Kadam, Megha, and Avinash Dhole. "Brain tumor detection using GLCM with the help of KSVM." International Journal of Engineering and Technical Research 7.2 (2017).
[21] Hussain, Ashfaq, and Ajay Khunteta. "Semantic Segmentation of Brain Tumor from MRI Images and SVM Classification using GLCM Features." 2020 Second International Conference on Inventive Research in Computing Applications (ICIRCA). IEEE, 2020.